Electronic Supplementary Material (ESI) for New Journal of Chemistry.
This journal is © The Royal Society of Chemistry and the Centre National de la Recherche Scientifique 2022

Supporting Information

Preparation of N/O-codoped quinoline pitch-based porous carbons for high-quality supercapacitor electrode

Zijian Yang, Qingjie Fan, Shiquan Lai*, Li Yue, Junxia Cheng, Yaming Zhu, Xuefei Zhao

School of Chemical Engineering, University of Science and Technology Liaoning, Qianshan Middle Road 185, Anshan 114051, Liaoning, China

**Corresponding author E-mail*: yuelilsq@163.com

1 Experimental section

1.1 Preparation of QLP-based porous carbons

QLP-based porous carbons (QLP-PCs) were prepared by the following process. The QLP without purification was thermally transformed into semi-coke at 450 ^{o}C for 2h. The resultant coke was crushed to a particle size less than 74 μm. 1g coke powder and 3g KOH were added into a beaker with 20 mL deionized water and magnetically stirred for 6 h. The obtained slurry was transferred into a nickel crucible and kept at 140 ^{o}C for 12h to fully remove moisture, then activated for 2 h at different temperatures (650, 700, 750 and 800 ^{o}C) in a tube furnace under a N_2 atmosphere. Finally, the activated samples were washed with 2 M H_2SO_4, rinsed with deionized water, and dried for 24 h at 110 ^{o}C.

1.2 Electrochemical measurements

Preparation of electrode sheet: QLP-PC powder (the mass was 4mg in three-electrode, 2 mg in device, respectively.), acetylene black and 5% PTFE in the mass ratio of 8:1:1 were mixed evenly with a small amount of ethanol until a slurry was formed. Hereafter, the resulting slurry was coated onto the nickel foam (1×1 cm^2) and allowed to dry at 80 °C in a vacuum oven for 12h. Finally, the electrode sheet of nickel foam was prepared under the pressure of 10 MPa, and then immersed subsequently in aqueous electrolyte (6 M KOH) for 12 h to ensure the internal channel was completely filled by the electrolyte.

Assembly of button-type supercapacitor cell: Firstly, the circular electrode sheet (12 mm in diameter, 0.12-0.14 mm in thickness) was prepared according to the manufacturing method of electrode sheet, and the obtained circular electrode sheet was immersed in 6 M KOH for 12 h. Subsequently, according to the sequence of battery shell, electrode sheet, electrolyte (6 M KOH), separator (polyethylene, Φ16 mm) composite diaphragm, electrolyte, electrode sheet and battery shell, the assembled button-type supercapacitor (as shown in Fig. S1) was made by compacting the battery shell under a pressure of 10 MPa.

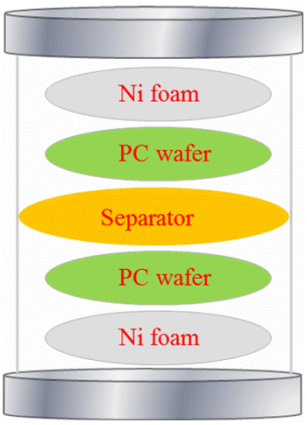

Fig. S1 Schematic diagram of the assembled button-type supercapacitor cell.

In the three-electrode system, the specific capacitance (C_s, F g^{-1}) was calculated from the discharge data of GCD based on the following equation [S1]:

$$C_s = \frac{I\Delta t}{m\Delta V} \quad \text{(S1.1)}$$

where I, Δt, ΔV and m are the constant current (A), discharge time (s), voltage change (V) and the mass (g) of active material in the electrode, respectively.

In the symmetrical supercapacitor cell, the specific capacitance (C_{cell}, F g^{-1}), energy density E_{cell} (Wh kg^{-1}) and power density P_{cell} (W kg^{-1}) of the cell can be calculated by the following equations [S1, S2]:

$$C_{cell} = \frac{I\Delta t}{m\Delta V} \quad \text{(S1.2)}$$

$$E_{cell} = \frac{C_{cell}(\Delta V)^2}{2\times 3.6} \quad \text{(S1.3)}$$

$$P_{cell} = \frac{E_{cell}}{\Delta t}\times 3600 \quad \text{(S1.4)}$$

where I, Δt, ΔV and m are the constant current (A), discharge time (s), voltage change (V) and the total mass (g) of active material in two electrodes, respectively.

2 Results and discussion

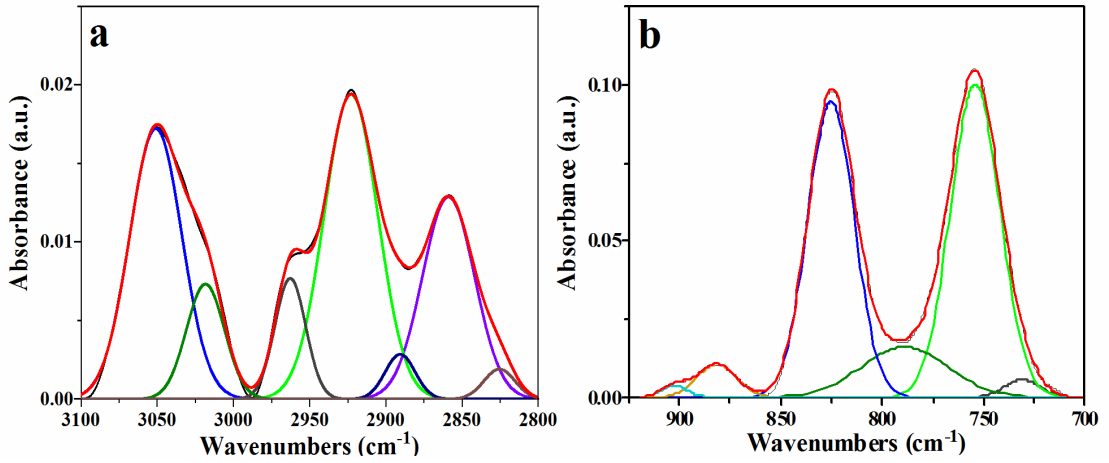

Fig. S2 Fitted spectra of the as-synthesized QLP in the range of 3100-2800 cm^{-1} (a) and 1000-700 cm^{-1} (b)

Fig. S2 presents the fitted spectra in the range of 3100-2800 cm^{-1} and 1000-700 cm^{-1}, respectively. The aromacity index (I_{ar}), the ortho-substitution index (I_{os}) and the aliphatic side chain index (CH_3/CH_2) of the as-synthesized QLP were calculated by the following equations based on their integrated

absorbance peak areas [S3-S5]:

$$I_{ar} = \mathrm{Abs}_{3050}/(\mathrm{Abs}_{3050}+\mathrm{Abs}_{2920}) \quad \text{(S2.1)}$$

$$\mathrm{CH_3/CH_2} = \mathrm{Abs}_{2950}/\mathrm{Abs}_{2920} \quad \text{(S2.2)}$$

$$I_{os} = \mathrm{Abs}_{750}/(\mathrm{Abs}_{880}+\mathrm{Abs}_{840}+\mathrm{Abs}_{814}+\mathrm{Abs}_{750}) \quad \text{(S2.3)}$$

Fig. S3 shows the other two PLM photos of the QLP-derived coke. According to the classification standards in Table S1, the volume content of each optical texture was obtained by counting about 200 valid points from these PLM photos. The optical texture index (OTI) of the QLP-derived coke was calculated by the following equation:

$$\mathrm{OTI} = \sum f_i(OTI)_i \quad \text{(S2.4)}$$

Where f_i and $(OTI)_i$ are the content of each optical texture and its corresponding OTI, respectively.

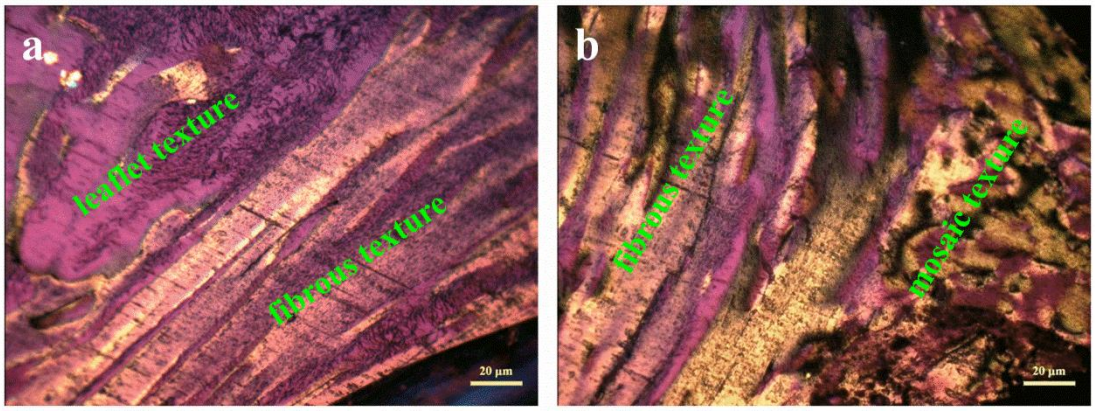

Fig. S3 POM photos (a, b) of the QLP-derived coke.

Table S1 The classification standards of each optical texture in coke and corresponding optical texture index (OTI) [S6, S7].

Optical organization	Length (μm)	Width (μm)	OTI index
leaflet texture	≥10	≥10	20
incompletely fibrous texture	10-30	<10	50
completely fibrous texture	≥30	<10	100
fragmental texture	<10	<10	0
fine mosaic texture	<1	<1	1
medium mosaic texture	1-5	1-5	3
coarse mosaic texture	5-10	5-10	7

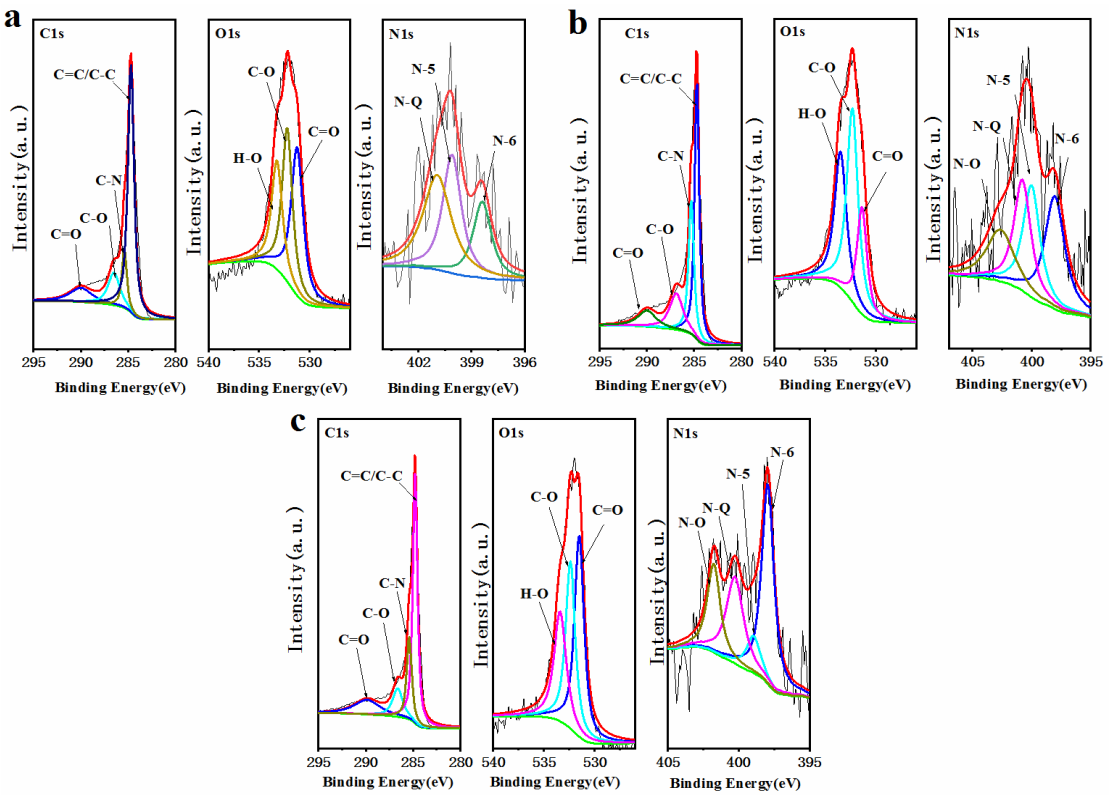

Fig. S4 High-resolution C1s, O1s and N1s XPS spectra of (a) QLP-PC-650, (b) QQLP-PC-750 and (c) QLP-PC-800.

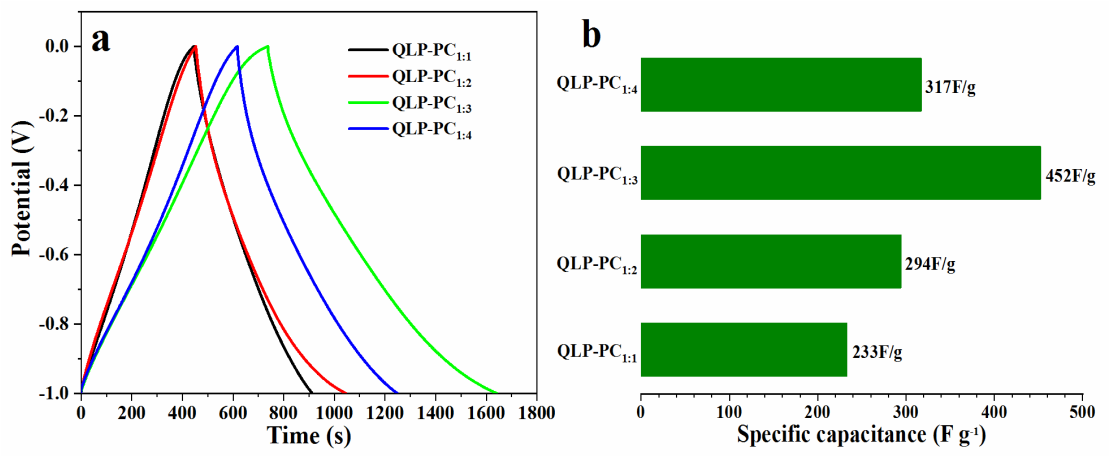

Fig. S5 GCD curves at a current density of 0.5 A/g (a) and specific capacitance (b) of QLP-PCs prepared using different carbon-alkali ratio at 700 ^{o}C. The subscript x in the QLP-PC$_x$ represents the carbon-alkali ratio.

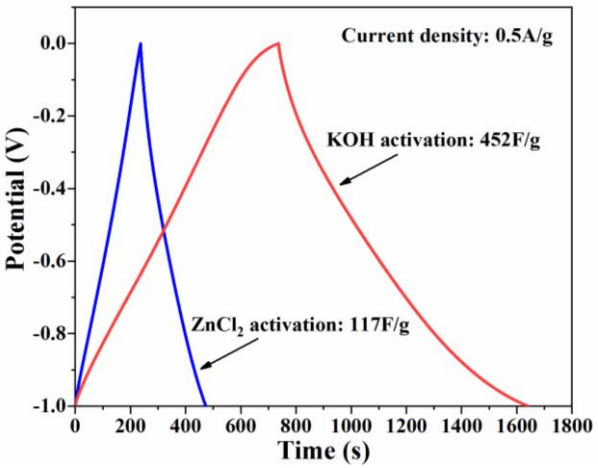

Fig. S6 The GCD curves of QLP-PCs prepared by KOH and $ZnCl_2$ activation under same conditions, respectively.

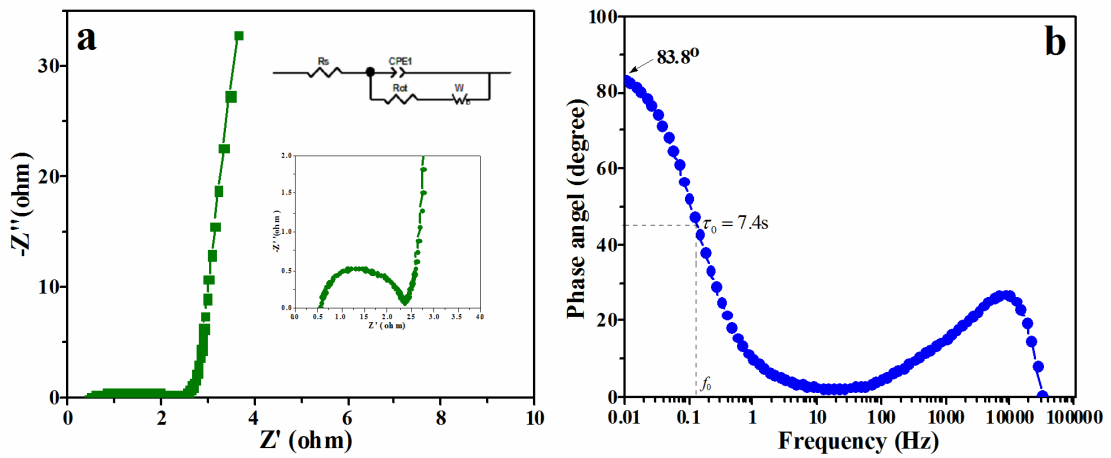

Fig. S7 The Nyquist plot (a) and the Bode plot (b) of the QLP-PC-700 based cell

R_s and R_{ct} are obtained by fitting the equivalent circuit of Fig. S7a.

Supplementary References

[S1] Y. W. Chi, C. C. Hu, H. H. Shen, K. P. Huang, A new approach for high-voltage electrical double-layer capacitors using vertical graphene nanowalls with and without nitrogen doping, Nano. Lett. 16 (2016) 5719-5727.

[S2] Q. S. Wang, Y. F. Zhang, J. Q. Xiao, H. M. Jiang, X. J. Li, C. G. Meng, A novel ordered hollow spherical nickel silicate–nickel hydroxide composite with two types of morphologies for enhanced electrochemical storage performance, Mater. Chem. Front. 3 (2019) 2090-2101.

[S3] Y. M Zhu, X. F. Zhao, L. J. Gao, J. Lv, J. X. Cheng, S. Q. Lai, Properties and micro-morphology of primary quinoline insoluble and mesocarbon microbeads, J. Mater. Sci. 51 (2016) 8098–8107.

[S4] C. Russo, F. Stanzione, A. Tregrossi, A. Ciajolo, Infrared spectroscopy of

some carbon-based materials relevant in combustion: Qualitative and quantitative analysis of hydrogen, Carbon, 74 (2014) 127-138.

[S5] M. D. Guillén, M. J. Iglesias, A. Dominguez, C. G. Blanco, Semiquantitative FTIR analysis of a coal tar pitch and its extracts and residues in several organic solvents, Energy & Fuels, 6 (1992) 518-525.

[S6] C. S. Hu, H. Y. Chu, Y. M. Zhu, Y. L. Xu, J. X. Cheng, L. J Gao, S. Q. Lai, X. F. Zhao, Differences and correlations between microstructure and macroscopic properties of mesophase cokes derived from the components of high temperature coal tar pitch, Fuel 310 (2022) 122330.

[S7] K. Chen, H. Zhang, U. K. Ibrahim, W. Y. Xue, H. Liu, A. Guo, The quantitative assessment of coke morphology based on the Raman spectroscopic characterization of serial petroleum cokes, Fuel 246 (2019) 60-68.